

**NASA TECHNICAL NOTE**



**NASA TN D-5047**

*c.1*

**NASA TN D-5047**



LOAN COPY: RETURN TO  
AFWL (WLIL-2)  
KIRTLAND AFB, N MEX

**FULL-SCALE INVESTIGATION OF  
THE AERODYNAMIC CHARACTERISTICS  
OF A SAILWING OF ASPECT RATIO 5.9**

*by Marvin P. Fink*

*Langley Research Center*

*Langley Station, Hampton, Va.*



FULL-SCALE INVESTIGATION OF THE AERODYNAMIC CHARACTERISTICS  
OF A SAILWING OF ASPECT RATIO 5.9

By Marvin P. Fink

Langley Research Center  
Langley Station, Hampton, Va.

NATIONAL AERONAUTICS AND SPACE ADMINISTRATION

---

For sale by the Clearinghouse for Federal Scientific and Technical Information  
Springfield, Virginia 22151 - CFSTI price \$3.00

FULL-SCALE INVESTIGATION OF THE AERODYNAMIC CHARACTERISTICS  
OF A SAILWING OF ASPECT RATIO 5.9

By Marvin P. Fink  
Langley Research Center

SUMMARY

An investigation has been conducted in the Langley full-scale tunnel to determine the aerodynamic characteristics of a full-scale model employing a sailwing having a wing aspect ratio of 5.9. The wing had a rigid leading-edge spar, rigid root and wing-tip ribs, a trailing-edge cable stretched between these ribs, and a fabric covering stretched between the leading and trailing edges. Included in the investigation were tests to determine the effect of a round leading edge as well as a D-spar leading edge on the aerodynamic characteristics of the model. Also, the effects of geometric dihedral on the lateral characteristics were determined.

The aerodynamic characteristics of the sailwing compared favorably with those of a conventional wing in terms of maximum lift and maximum lift-drag ratio. The round-spar leading-edge configuration had higher lift coefficients but lower values of maximum lift-drag ratio than those of the D-spar configuration. Increased dihedral caused a decrease in maximum lift for both configurations, produced the expected increase in effective dihedral, and gave little effect on the directional stability characteristics.

INTRODUCTION

There have been many schemes in which the conventional rigid type of construction of an airplane wing was replaced with a minimum-structure fabric surface in an effort to achieve structural simplicity. One such device, first conceived as an advanced sail for a boat, was later converted to an airplane wing. This type of wing uses a single spar as the wing leading-edge and main load-carrying member, ribs only at the tip and root, a wire trailing edge stretched between the ribs, and a fabric envelope to form the wing surface. A device of this type, called a sailwing (devised at Princeton University), has been tested in the Langley full-scale tunnel to evaluate the aerodynamic characteristics of a wing of this simplified type of structure.

The results of one investigation in which an aspect-ratio-11.5 full-scale sailwing was employed on a complete airplane configuration are presented in reference 1. The

present investigation was conducted on an aspect-ratio-5.9 full-scale sailwing with the wing mounted on an apparatus that would give a minimum of aerodynamic interference so that the results would be approximately those for a wing alone. The investigation included tests to study the effects of a round leading edge as compared with a D-spar leading edge on the longitudinal characteristics of the model. In addition, tests were also conducted to determine the effects of changes in geometric dihedral on the lateral stability characteristics of the model.

## SYMBOLS

Figure 1 shows the stability-axis system used in the presentation of the data and the positive directions of the forces, moments, and angles. The data are computed about the moment center shown in figure 2 which is located at the  $0.18\bar{c}$  station. Measurements for this investigation were taken in the U.S. Customary System of Units. Equivalent values are indicated herein in the International System of Units (SI) in the interest of promoting the use of this system in future NASA reports. Details concerning the use of SI may be found in reference 2.

$C_D$	drag coefficient, $\frac{\text{Drag}}{qS}$
$C_L$	lift coefficient, $\frac{\text{Lift}}{qS}$
$C_l$	rolling-moment coefficient, $\frac{\text{Rolling moment}}{qSb}$
$C_m$	pitching-moment coefficient, $\frac{\text{Pitching moment}}{qS\bar{c}}$
$C_n$	yawing-moment coefficient, $\frac{\text{Yawing moment}}{qSb}$
$C_Y$	side-force coefficient, $\frac{\text{Side force}}{qSb}$
$C_{l\beta} = \frac{\partial C_l}{\partial \beta}$	
$C_{n\beta} = \frac{\partial C_n}{\partial \beta}$	
A	aspect ratio
b	wing span, 23.3 feet (7.10 meters)
c	wing chord, feet (meters)

$\bar{c}$	mean aerodynamic chord, 3.98 feet (1.21 meters), $\bar{c} = \frac{2}{S} \int_0^{b/2} c^2 dy$
e	wing efficiency factor
L/D	lift-drag ratio
q	free-stream dynamic pressure, pounds/square foot (newtons/meter <sup>2</sup> )
S	wing area, 92.8 square feet (8.4 meter <sup>2</sup> )
V	free-stream velocity, feet/second (meters/second)
X,Y,Z	coordinate axes
y	spanwise distance, feet (meters)
$\alpha$	angle of attack, degrees
$\beta$	sideslip angle, degrees
$\delta_f$	flap deflection, degrees
$\lambda$	taper ratio
$\Gamma$	dihedral angle, degrees

## MODEL AND TESTS

### Model

The configuration tested in the current investigation was a full-scale wing. A three-view drawing showing the general arrangement of the model and the principal dimensions is given in figure 2. The framework used to support the wing and bridle assembly was of simple tubular construction and was designed to provide a rigid base for the wing without giving large interference effects on the wing. It is necessary to use some such wing support system in tests of a sailwing to provide attachment points for the various wires and struts that reinforce the wing. The wing had an aspect ratio of 5.9 and a taper ratio of 0.5. The wing construction consisted of a rigid leading-edge spar, a wire trailing edge, and rigid ribs at the wing tip and root. This framework was covered with

a fabric envelope which formed the upper and lower surfaces of the wing. The fabric was Dacron sailcloth with no treatment and was made taut by adjustable tension bridle wires attached to the trailing edge as shown in figure 2. The two leading-edge configurations tested, a D-spar and a round spar, are shown in figure 3. Figure 4 presents a photograph of the model mounted in the tunnel test section.

## Tests

Tests were made to determine the aerodynamic characteristics of the novel type of wing used on the model. The principal characteristics of interest were (1) lift and drag, (2) the static longitudinal and lateral stability and the effect of change of geometric dihedral and leading-edge shape on these characteristics. The tests were made in the Langley full-scale tunnel which is described in reference 3. The model was tested over an angle-of-attack range from  $-6.7^\circ$  to  $19.3^\circ$  at a tunnel velocity of about 63 ft/sec (19.2 m/sec) and over a range of sideslip angles of  $\pm 12^\circ$  for dihedral angles of  $0^\circ$ ,  $5^\circ$ , and  $10^\circ$ . A few tests were also made at tunnel velocities of 50 ft/sec (15.24 m/sec) and 75 ft/sec (22.86 m/sec) at zero sideslip. The bridle tension was held constant at 70 pounds (311 N) for all the tests except for a few specific tests in which the effect of bridle tension was investigated. The results have been corrected for airstream misalignment and the wing-support system tares. The wing-support system tares were determined by removing the wing from the mounting structure and measuring the forces and moments on the structure over the angle-of-attack range. All the tares were negligible except drag; and the drag tare was taken out of the total drag to obtain the wing drag. The wing drag includes the drag of the lift strut, bridle wires, and any support system interference drag, since these support and interference drag values could not be determined.

## DISCUSSION

### Longitudinal Characteristics

The basic longitudinal aerodynamic characteristics are given in figures 5 and 6. The general character of the lift curves is that their slopes are steep at low angles of attack and flattened at high angles of attack as was the case for the high-aspect-ratio sailing of reference 1. This characteristic results from the fact that at low lift coefficients, the camber of the wing increases with increasing lift as the fabric and wires stretch. At higher lift coefficients, the fabric is fully stretched and the camber does not change appreciably with increasing angle of attack and the lift-curve slope (for example, at  $C_L \approx 1.0$ ) is about 0.08 as compared with about 1.0 at a  $C_L \approx 0.5$ . The reason for the abrupt changes in lift-curve slope for the D-spar wing at lift coefficients of about 0.3 to 0.4 is not known. The characteristic shape of the pitching-moment curves is that they

show a negative slope  $\left(-\frac{dC_m}{dC_L}\right)$  at low lift coefficients and about zero slope at high lift coefficients. This characteristic evidently results from the fact that the camber is increasing, with a rearward shift of the aerodynamic loading, as lift increases in the low-lift range; but that at high lift the camber is approximately constant so that the loading does not continue to move rearward.

The effects of dynamic pressure on both the D-spar and round-spar leading-edge configuration are shown in figure 5. These data show that for both configurations increasing the dynamic pressure from 4.8 lb/ft<sup>2</sup> (230 N/m<sup>2</sup>) to 6.6 lb/ft<sup>2</sup> (316 N/m<sup>2</sup>) did not materially change maximum lift, the angle of attack for maximum lift ( $\alpha \approx 17^\circ$ ), or the lift-curve slope.

Figure 6 presents the effect of geometric dihedral angle on lift. These data show that maximum lift was proportionately lowered as dihedral was increased from  $\Gamma = 0^\circ$  to  $\Gamma = 10^\circ$  and are consistent with the trend shown in reference 4 for a hard wing. The lift coefficients are all based on the projected wing area for the wing with  $\Gamma = 0^\circ$ ; consequently, maximum lift would be expected to lower with dihedral. The lift reduction, however, seems to be considerably more than the reduction due to projected area, and may, in part, be attributed to the fact that wing stall started at a somewhat lower angle of attack with the higher dihedral angles.

A comparison of the aerodynamic characteristics for the D-spar and round-spar wings is presented in figure 7 for  $\Gamma = 5^\circ$ . The data of figure 7(a) show that the round-spar wing had higher lift than the D-spar wing over the entire positive lift range. It is also noted that the round-spar configuration had the higher drag and its lift-drag ratio, as shown in figure 7(b), was somewhat lower.

For all the foregoing tests, the bridle tension was held constant at 70 pounds. The data of figure 8 show that decreasing the bridle wire tension had little effect on the longitudinal characteristics, but removing the bridle altogether caused an increase in maximum lift and, at a given lift coefficient, a decrease in effective angle of attack of about  $2^\circ$ .

### Lateral Characteristics

The basic lateral data are shown in figures 9 and 10 plotted against sideslip angles for a range of angle of attack. These data are summarized in figures 11 and 12, in terms of the effective dihedral parameter  $(-C_{l_\beta})$  and the directional stability parameter  $C_{n_\beta}$  for the D-spar and the round-spar configurations. The values of  $C_{l_\beta}$  and  $C_{n_\beta}$  presented are the values obtained from the incremental differences between the moments at  $\pm 4^\circ$ . The data show that increased geometric dihedral caused an increase in  $-C_{l_\beta}$  for both configurations, and that the D-spar wing generally had higher values of  $-C_{l_\beta}$  for a given geometric dihedral than did the round-spar wing. The data of figure 12 show that

for angles of attack above the stall,  $\alpha = 19^\circ$ , the effective dihedral is decreased with increased  $\Gamma$  but the values of  $-C_{l\beta}$  were fairly high for all the conditions tested in the angle-of-attack range. The directional stability  $C_{n\beta}$  (as shown in fig. 11(b)) is not appreciably affected by an increase in geometric dihedral or by leading-edge shape.

### Comparison With Conventional Wing

Figures 13 to 15 were prepared to show the general relationship of some of the characteristics of the sailwing and a wing of conventional construction. Exact comparison is not intended in this report. In figure 13 the lift characteristics of both the D-spar and the round-spar wings are compared with the lift characteristics of a hard wing having an aspect ratio of 6 and an NACA 23012 airfoil. (See ref. 5.) It is noted that because of the cambering of the sailwing, the lift characteristics agree reasonably well with those of the hard wing with a  $0.20\bar{c}$  full-span flap deflected  $20^\circ$ . Maximum lift of the sailwing, however, is somewhat lower than that for the hard wing with the flap deflected. A comparison of  $L/D$  for the sailwing and rigid wing (fig. 14) shows that the sailwing attained maximum values of  $L/D$  of about 19 as compared with values of about 22 for the conventional wings, but that  $L/D$  of the D-spar sailwing was slightly higher than that of the conventional wing for values of  $C_L$  greater than about 0.7. The data of figure 15 show that the sailwing had considerably higher values of minimum drag than did the smooth conventional wind-tunnel model, but at angles where the sail attained camber and tautness the sailwing had lower drag than did the conventional wing. Over the linear portion of the drag polar, the sailwing had a span efficiency factor  $\left( e = \frac{C_L^2/C_D}{\pi A} \right)$  of about 0.90 as compared with 0.80 for the hard wing.

### CONCLUSIONS

An experimental investigation to determine the aerodynamic characteristics of a full-scale model employing the sailwing concept has been made and the following conclusions were drawn from the results of the investigation:

1. The sailwing attained values of maximum lift and maximum lift-drag ratio comparable with that of a similar conventional hard wing.
2. The shape of the wing leading edge had only small effects on the longitudinal and lateral characteristics of the sailwing. A round leading-edge configuration attained slightly higher lift coefficients but produced lower values of maximum lift-drag ratio.



3. Increasing the geometric dihedral caused a slight decrease in the value of maximum lift coefficient, produced the expected increase in effective dihedral, and had only a small effect on the directional stability characteristics.

Langley Research Center,  
National Aeronautics and Space Administration,  
Langley Station, Hampton, Va., January 6, 1969,  
126-13-01-60-23.

#### REFERENCES

1. Fink, Marvin P.: Full-Scale Investigation of the Aerodynamic Characteristics of a Model Employing a Sailwing Concept. NASA TN D-4062, 1967.
2. Mechtly, E. A.: The International System of Units - Physical Constants and Conversion Factors. NASA SP-7012, 1964.
3. DeFrance, Smith J.: The N.A.C.A Full-Scale Wind Tunnel. NACA Rep. 459, 1933.
4. Shortal, Joseph A.: The Effect of Tip Shape and Dihedral on Lateral-Stability Characteristics. NACA Rep. 548, 1935.
5. Anderson, Raymond F.: The Experimental and Calculated Characteristics of 22 Tapered Wings. NACA Rep. 627, 1938.

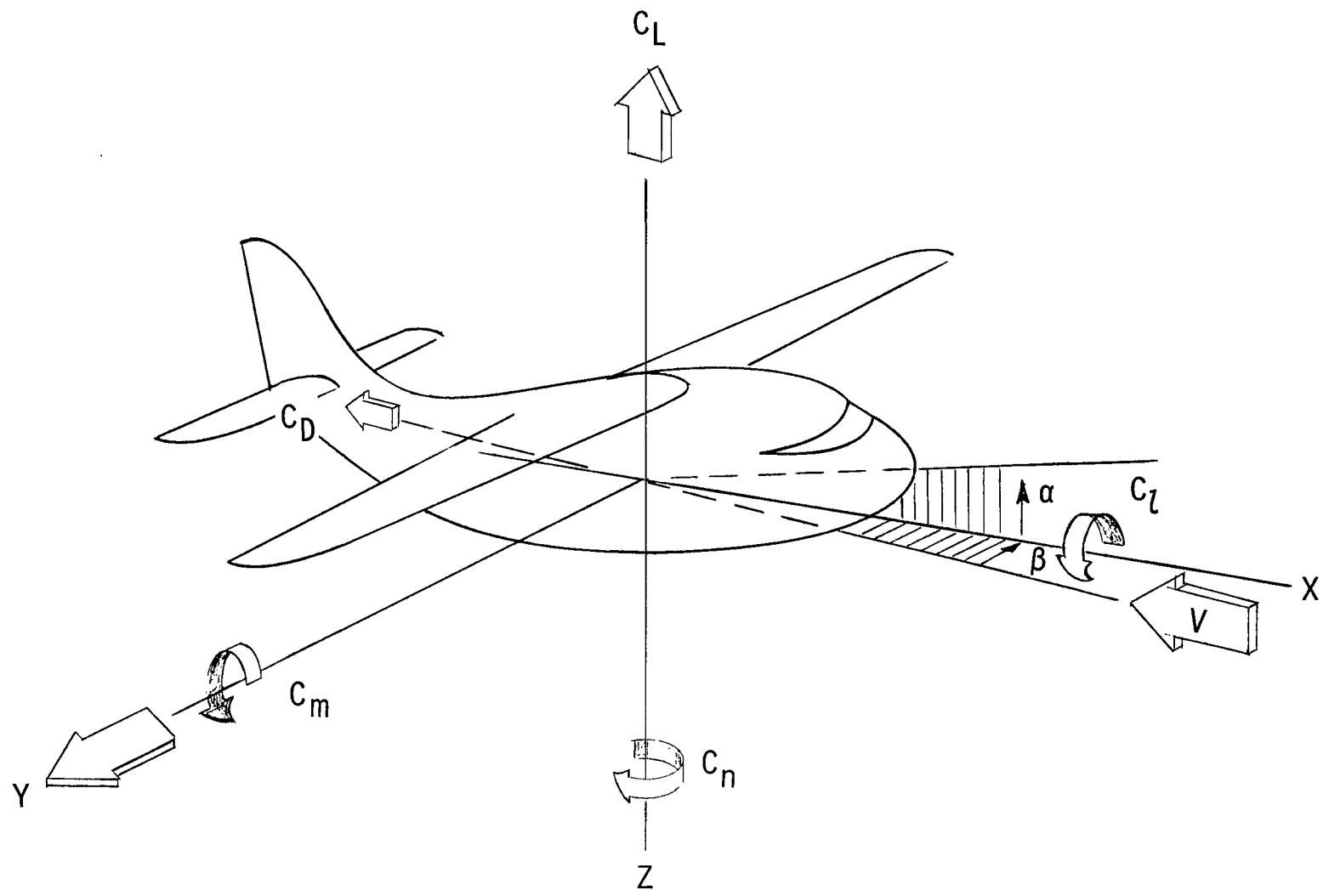


Figure 1.- System of axes and positive sense of angles, forces, and moments.

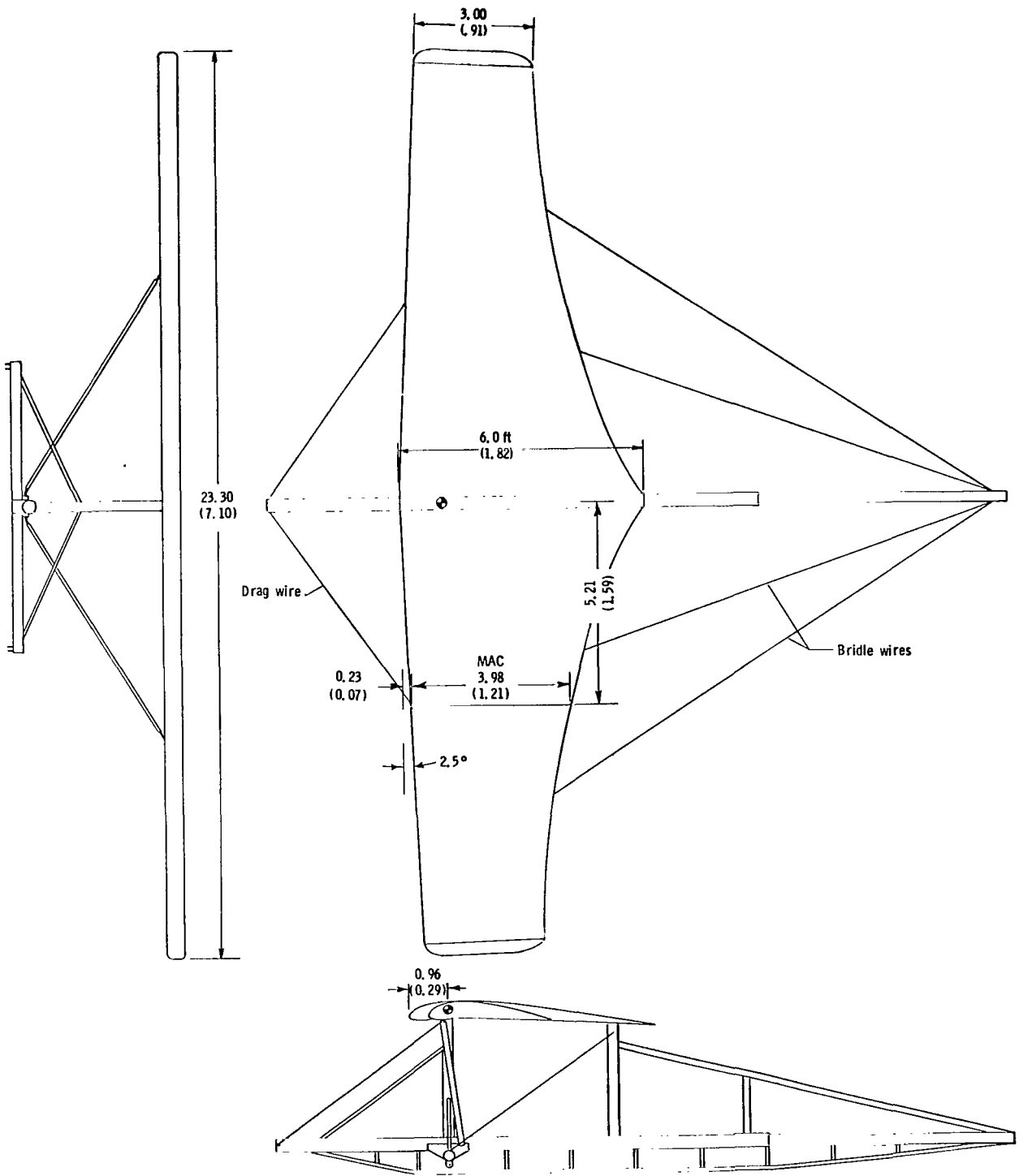
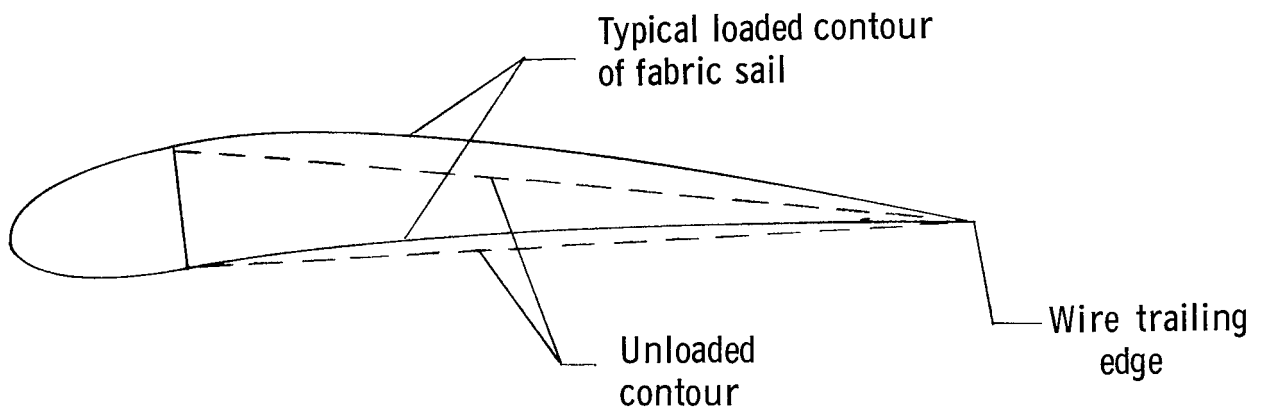


Figure 2.- Sketch of model. Dimensions are given in feet and parenthetically in meters.

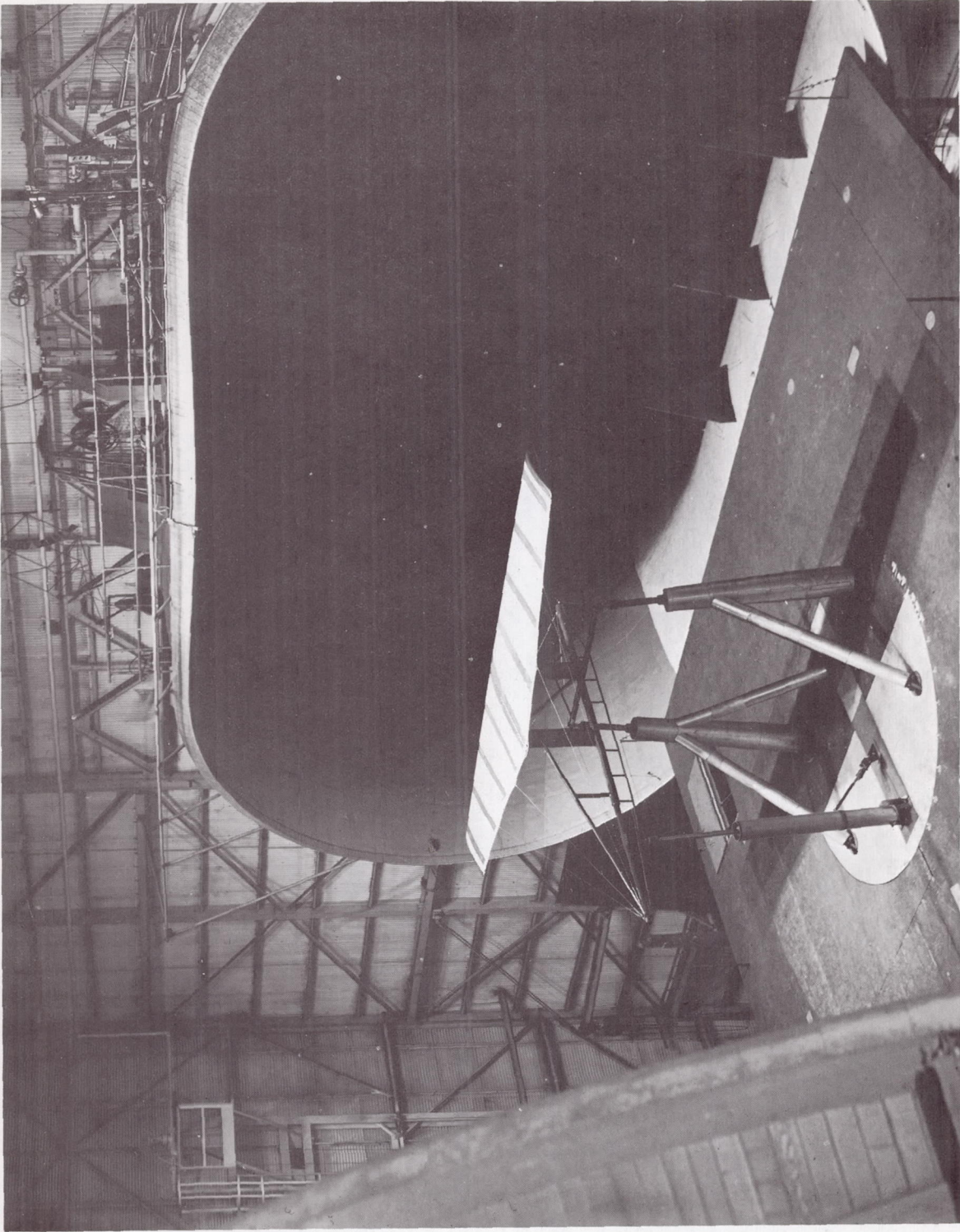


Round-spar configuration



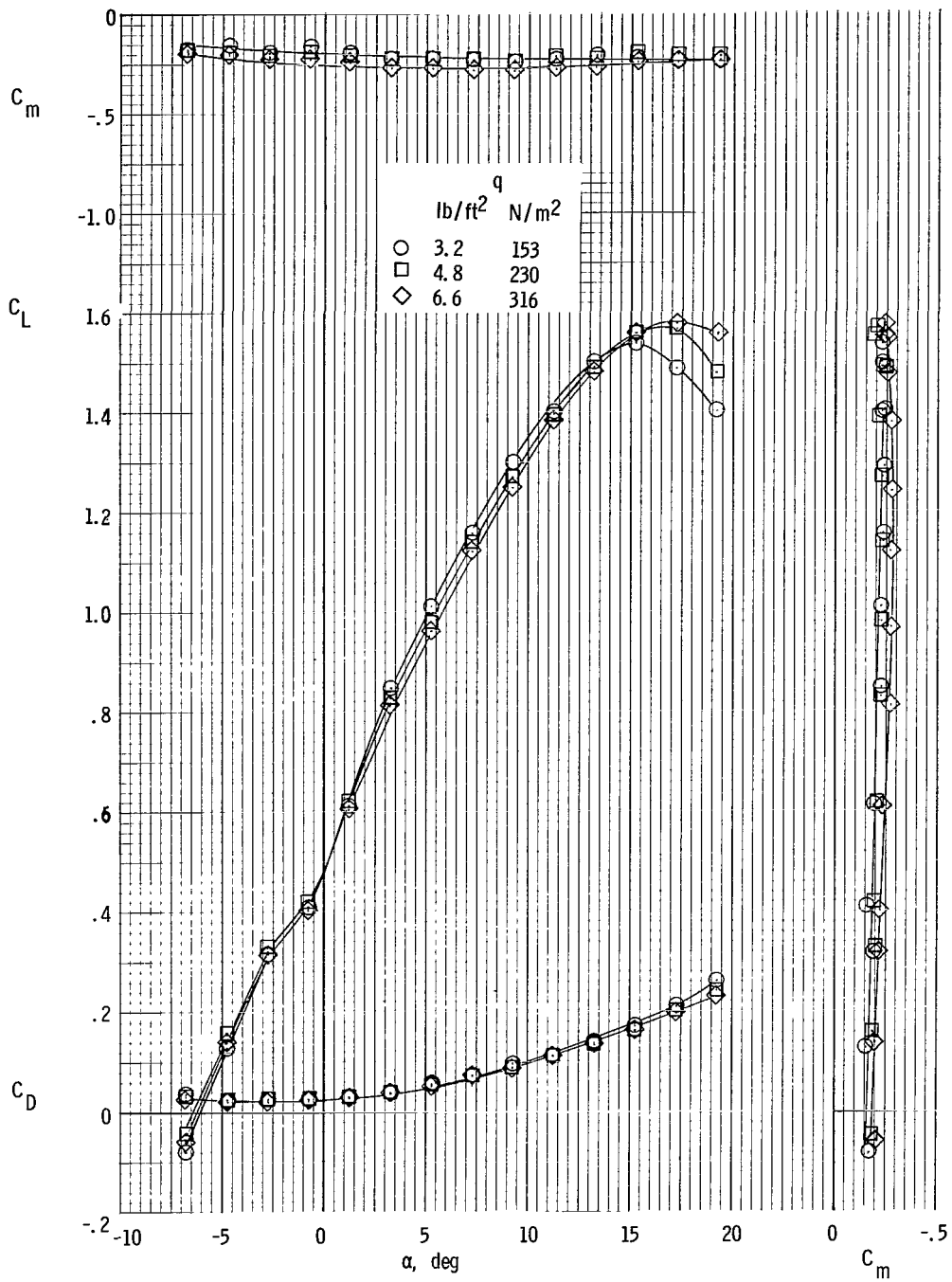
D-spar configuration

Figure 3.- Typical cross-sectional views of the D-spar and round-spar configurations.



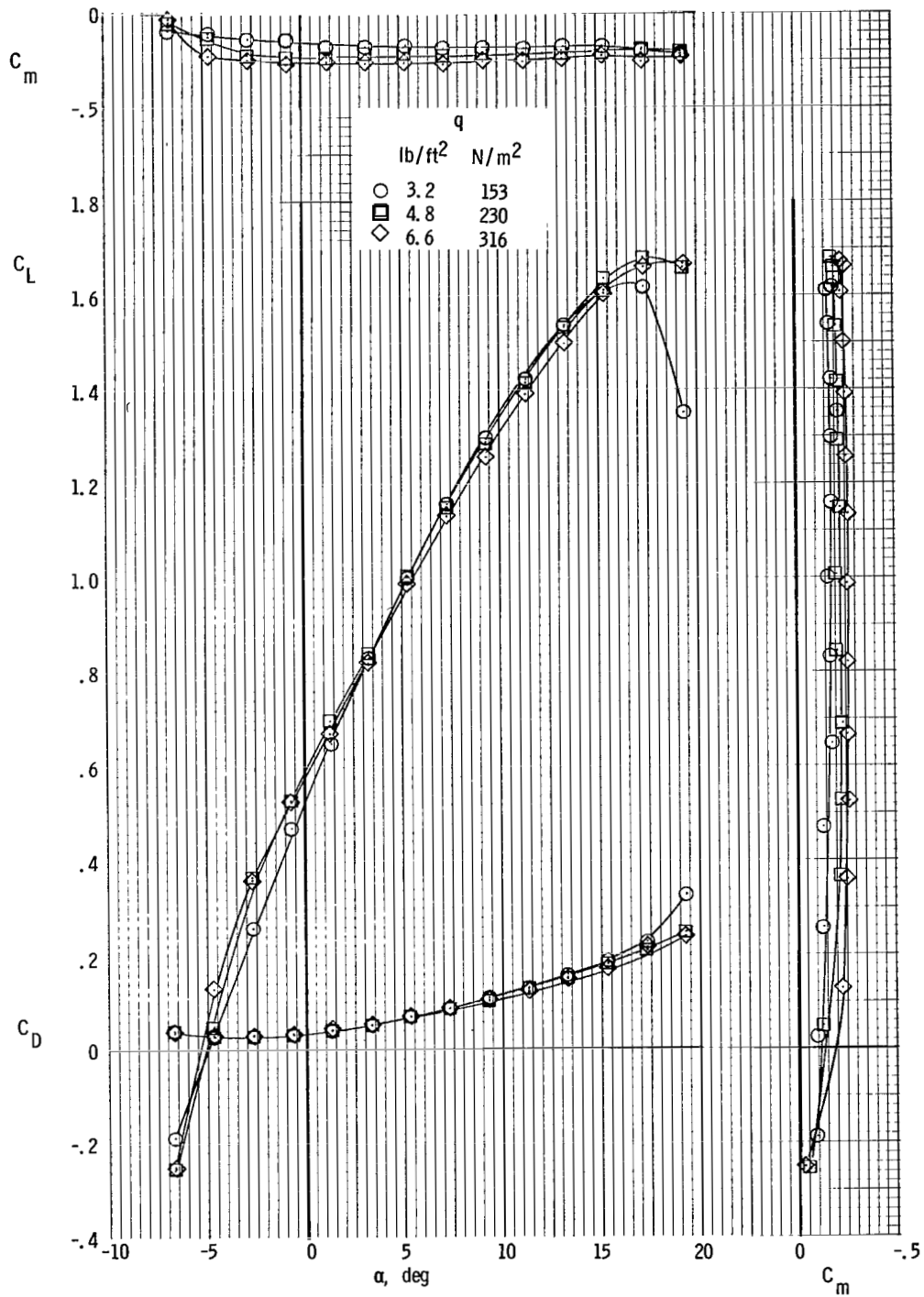
L-67-4246

Figure 4.- Photograph of model installed in tunnel.



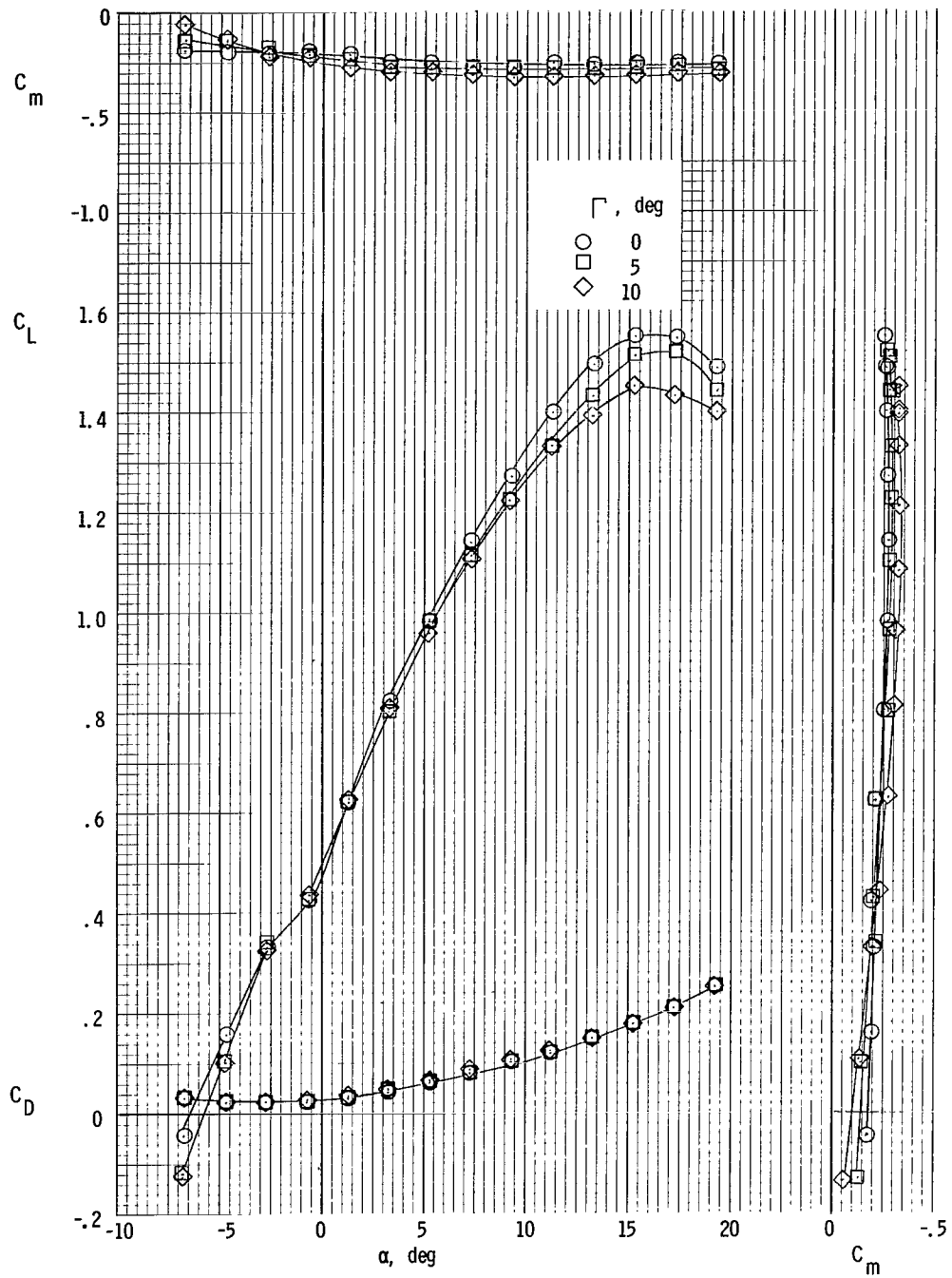
(a) D-spar configuration.

Figure 5.- Variation of the longitudinal aerodynamic characteristics with angle of attack for several dynamic pressures.  $\Gamma = 0^\circ$ .



(b) Round-spar configuration.

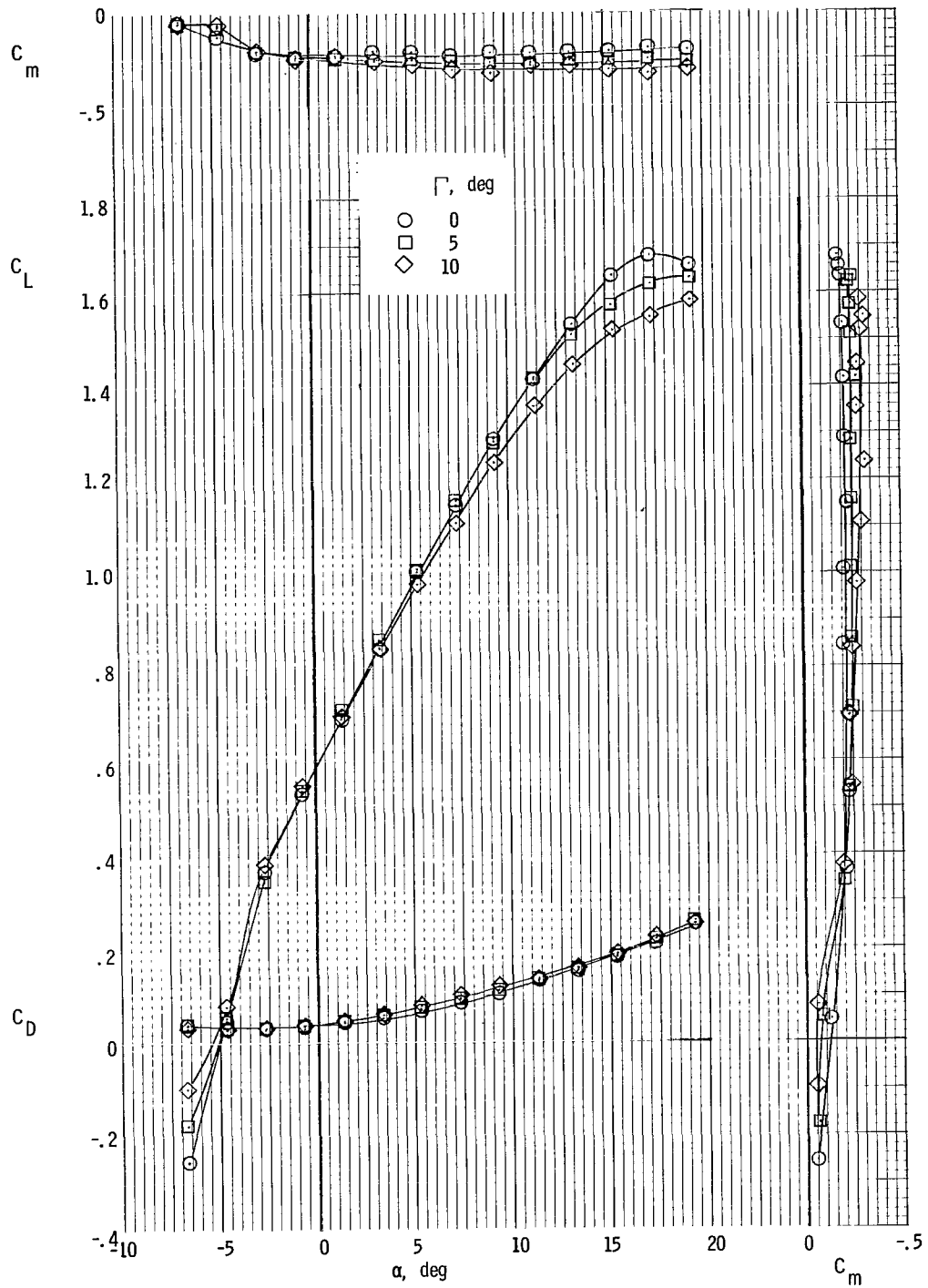
Figure 5.- Concluded.



(a) D-spar configuration.

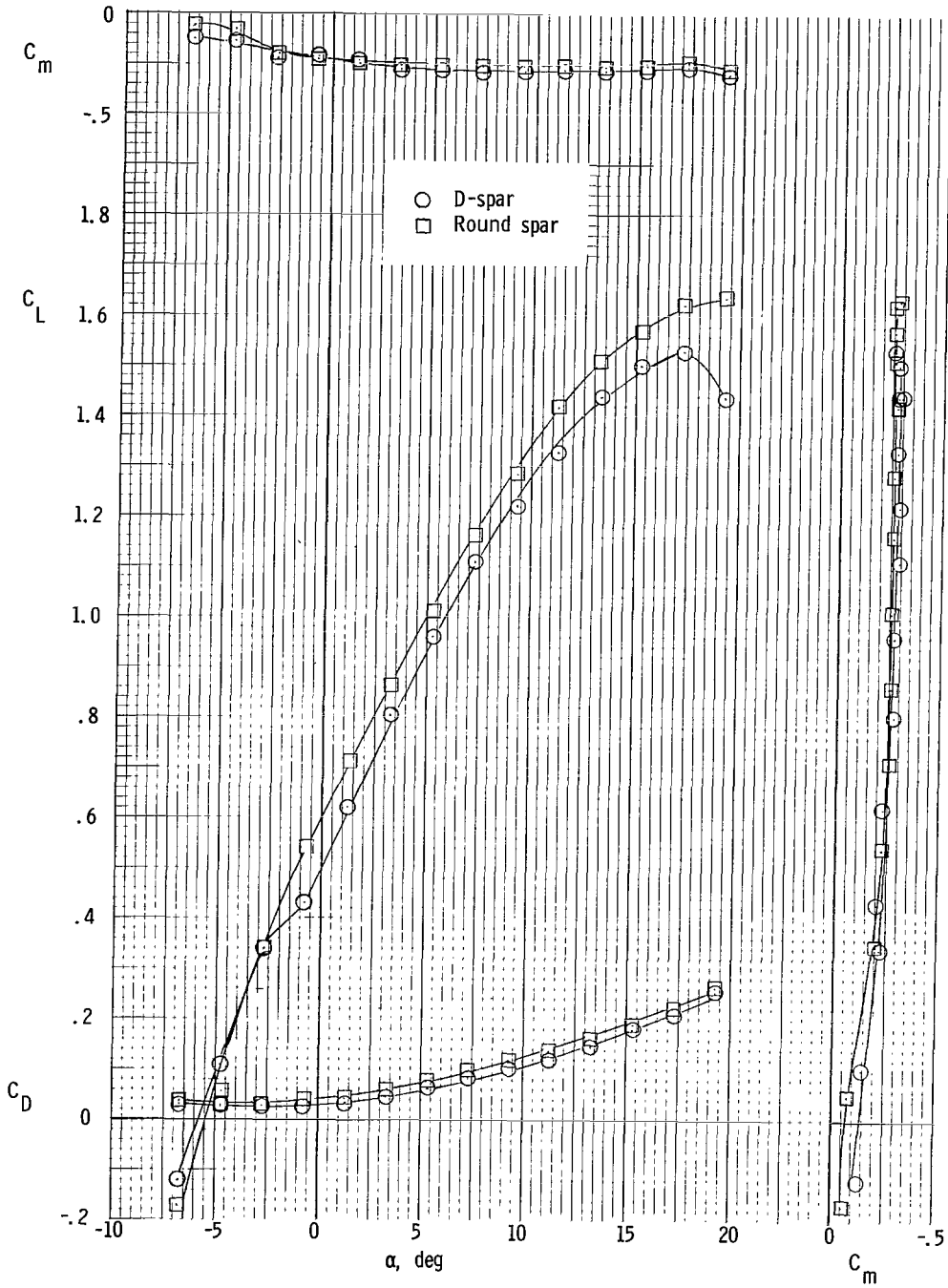
Figure 6.- Variation of the longitudinal aerodynamic characteristics with angle of attack for several dihedral angles.  $q = 4.8 \text{ lb/ft}^2$  ( $230 \text{ N/m}^2$ ).





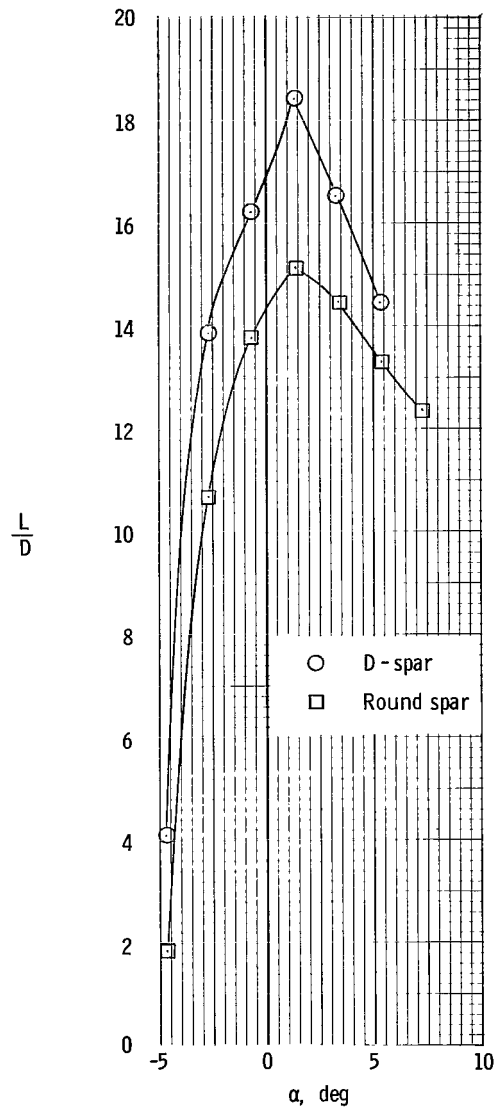
(b) Round-spar configuration.

Figure 6.- Concluded.



(a) Aerodynamic characteristics.

Figure 7.- Comparison of longitudinal aerodynamic characteristics and lift-drag ratio of the round-spar and D-spar configurations.  $\Gamma = 5^\circ$ ,  $q = 4.8 \text{ lb/ft}^2$  ( $230 \text{ N/m}^2$ ).



(b) Lift-drag ratio.

Figure 7. Concluded.

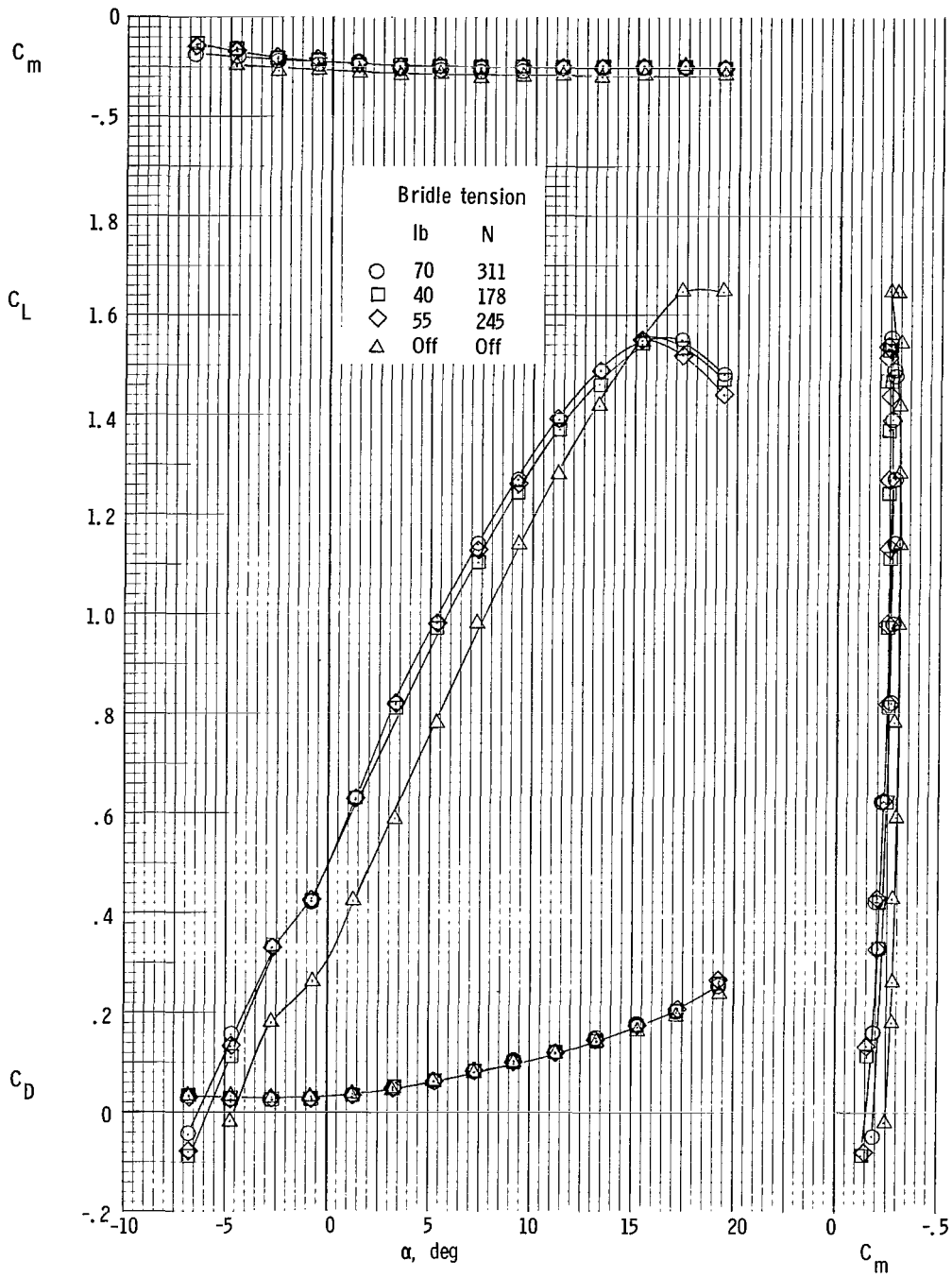
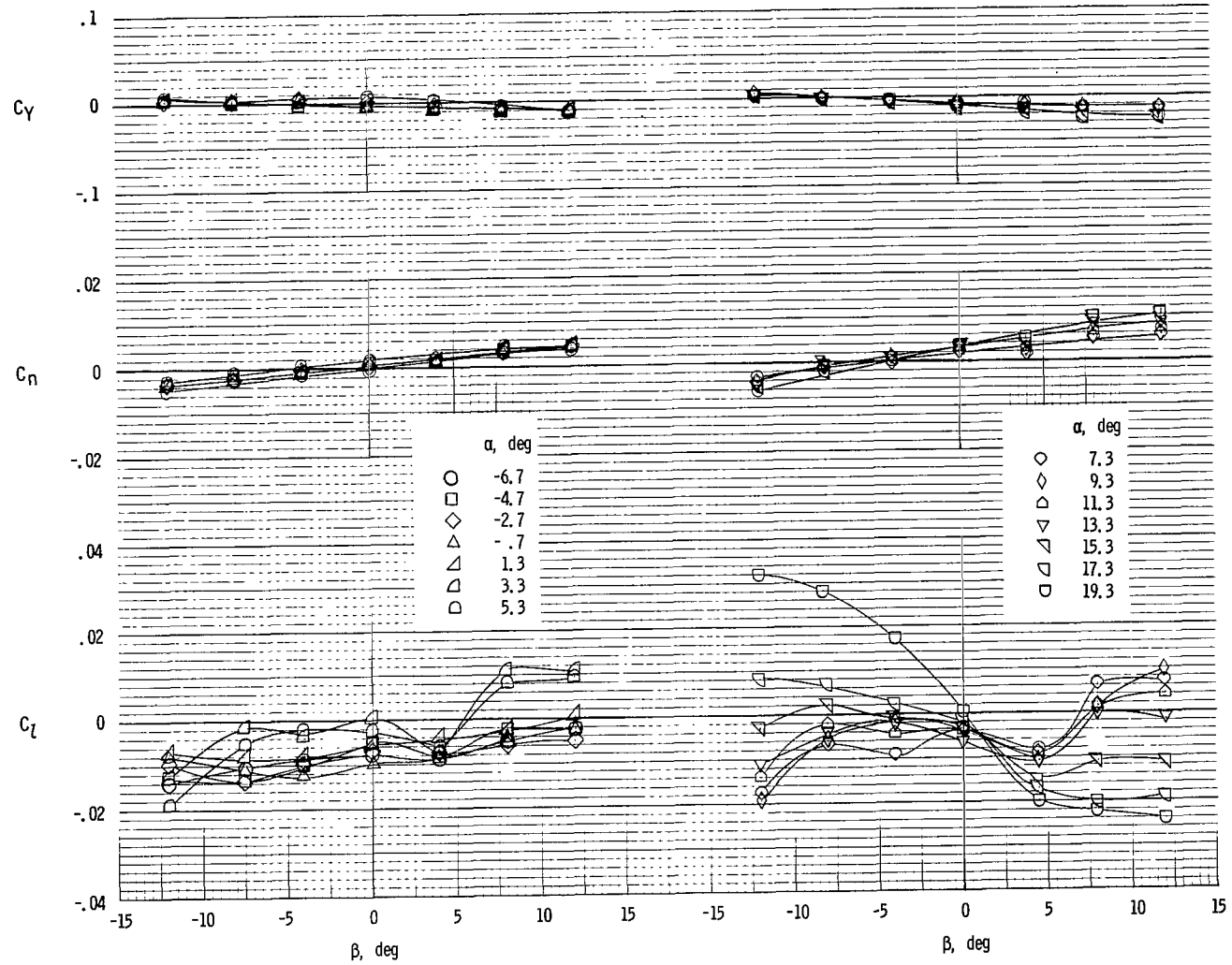
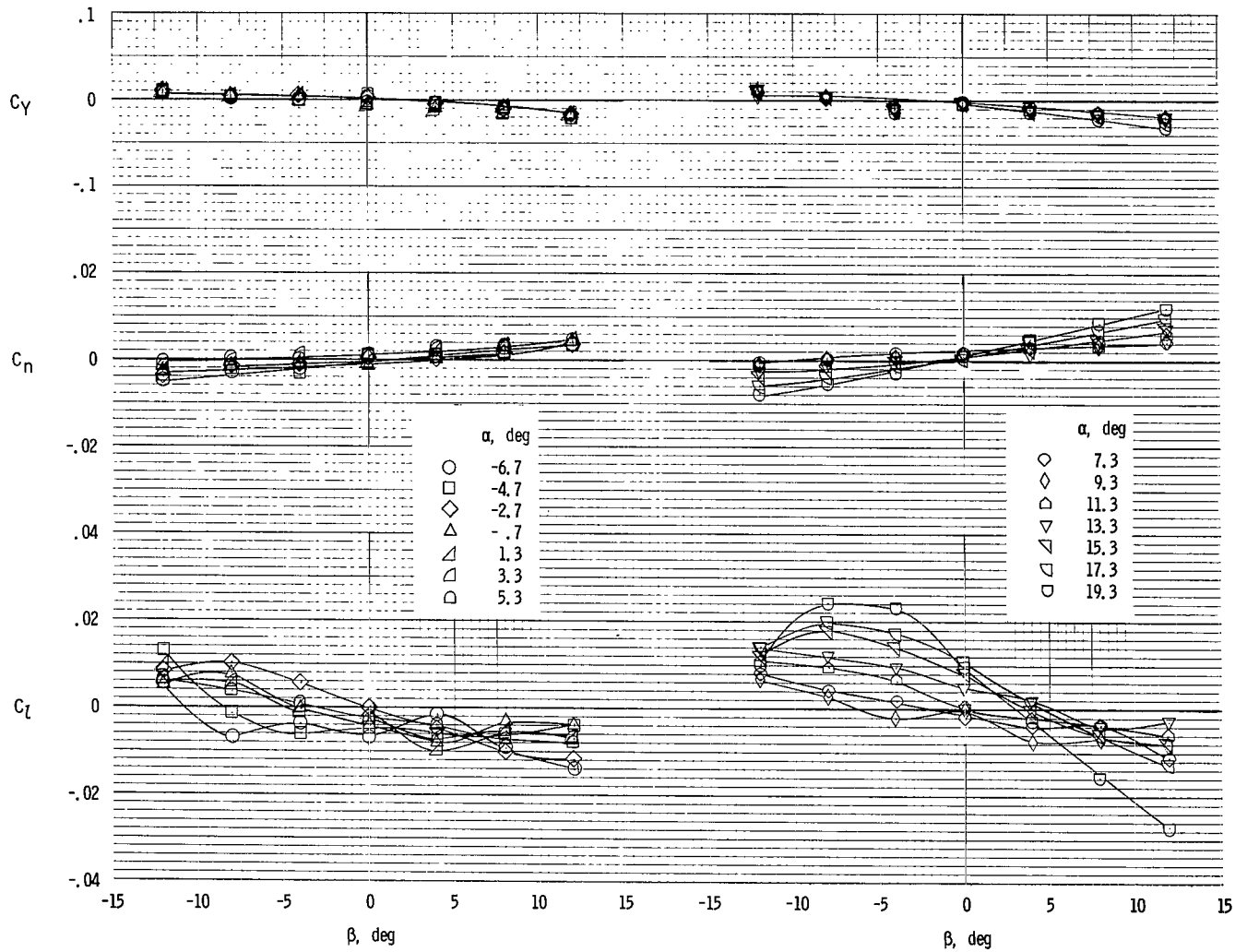


Figure 8. Effect of bridge wires on the longitudinal aerodynamic characteristics of the D-spar configuration.



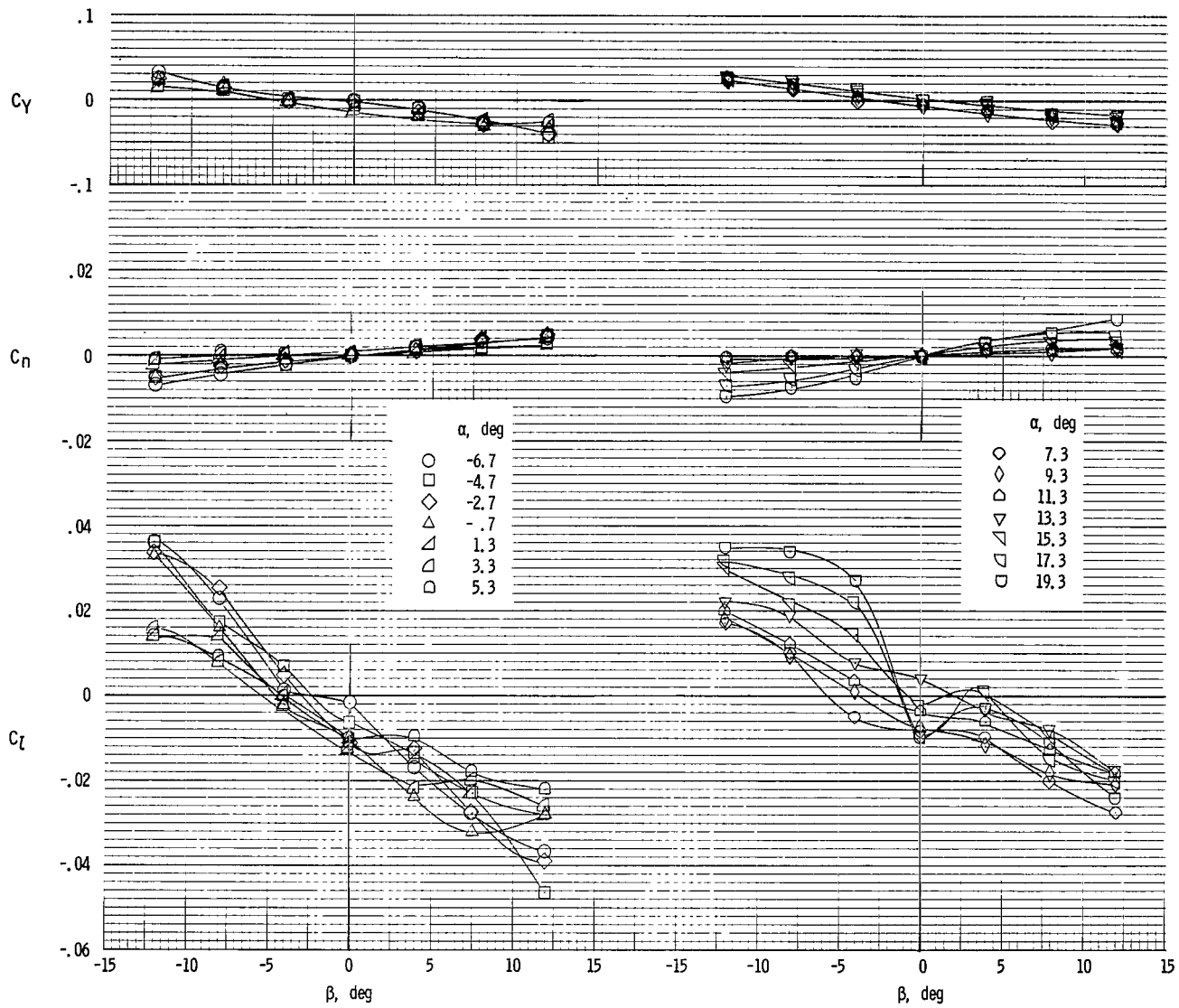
(a)  $\Gamma = 0^\circ$ .

Figure 9. Variation of the lateral characteristics of the wing with sideslip. D-spar configuration.



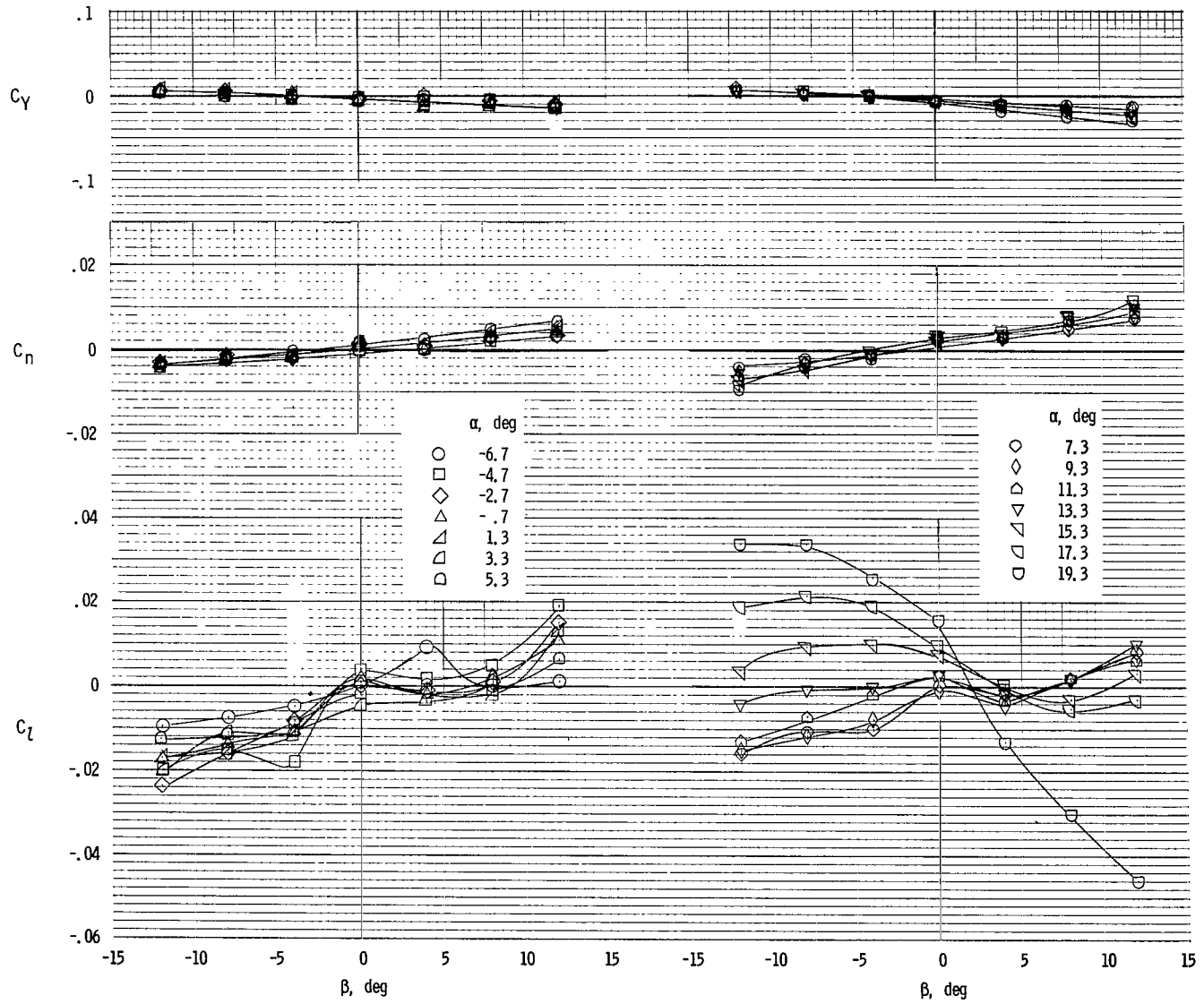
(b)  $\Gamma = 5^\circ$ .

Figure 9.- Continued.



(c)  $\Gamma = 10^\circ$ .

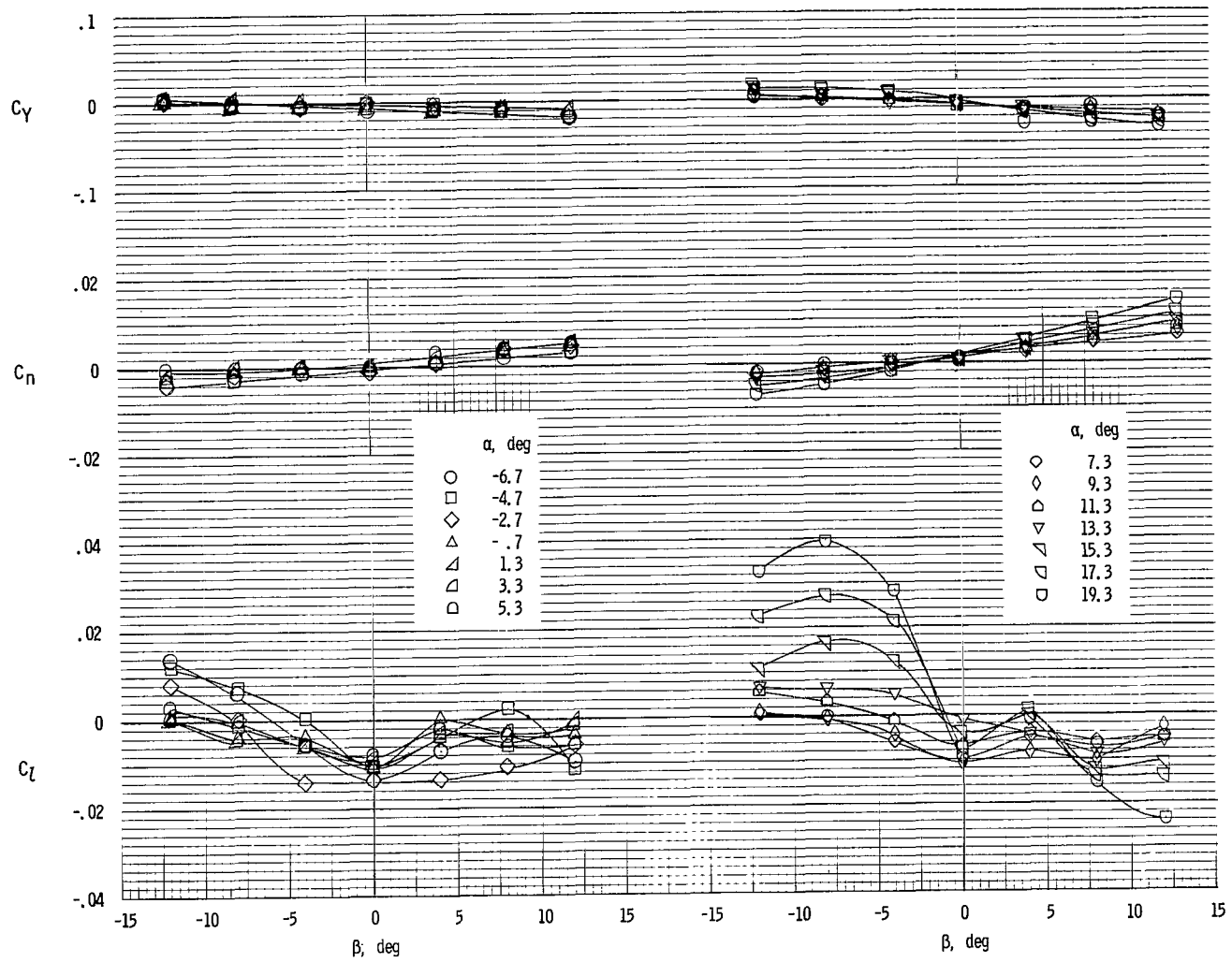
Figure 9.- Concluded.



(a)  $\Gamma = 0^\circ$ .

Figure 10.- Variation of the lateral characteristics of the wing with sideslip. Round-spar configuration.





(b)  $\Gamma = 5^\circ$ .

Figure 10.- Continued.

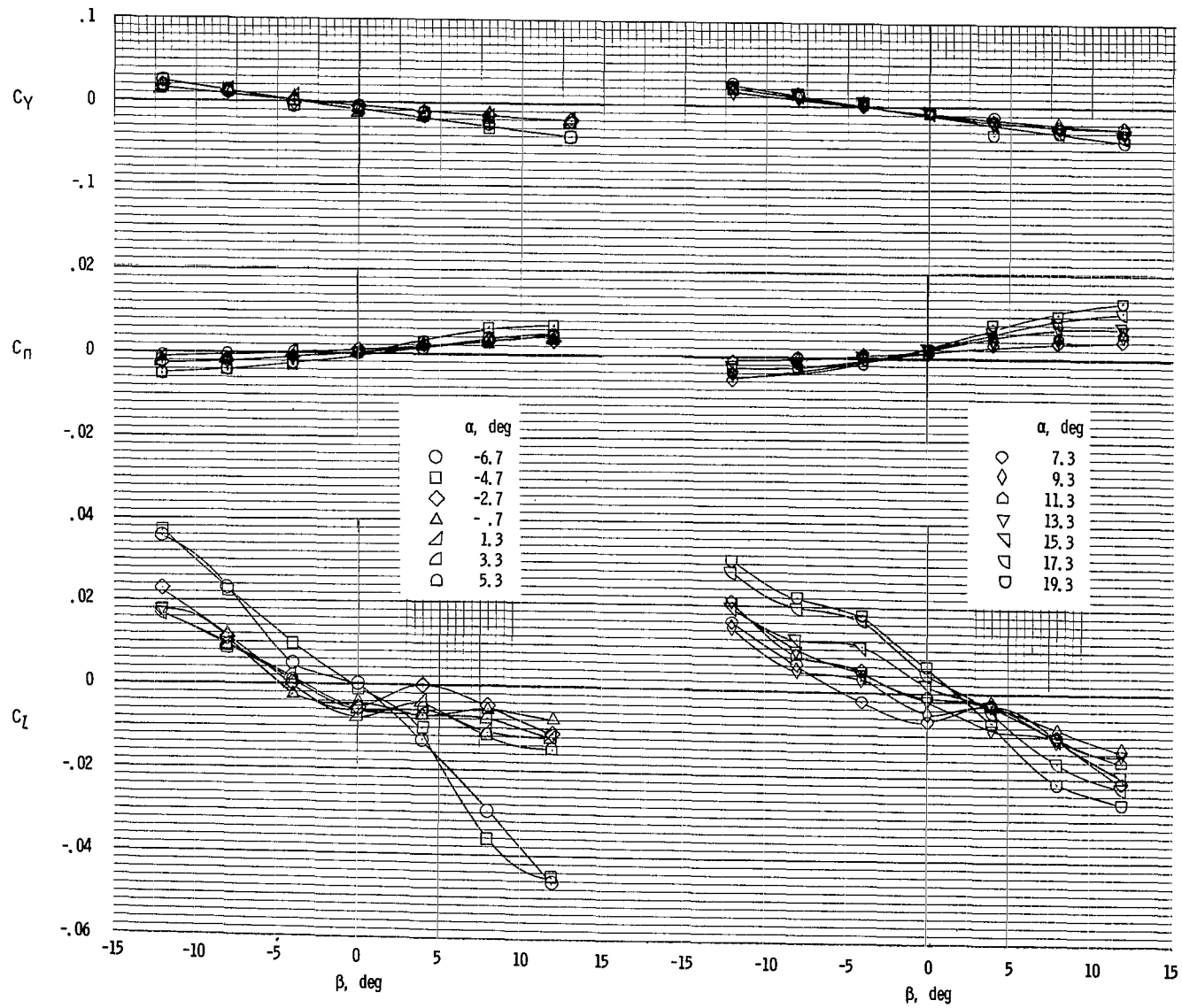
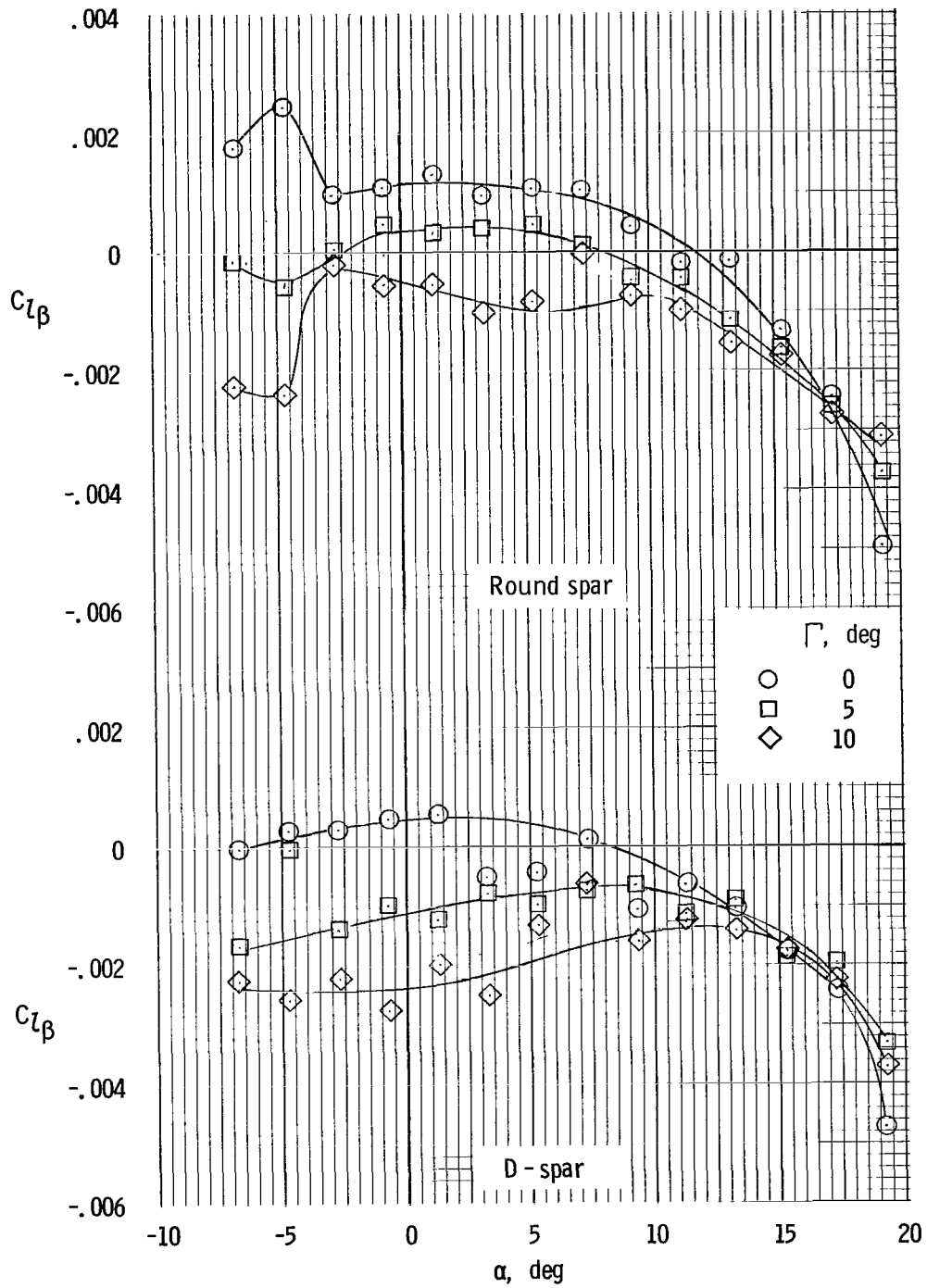
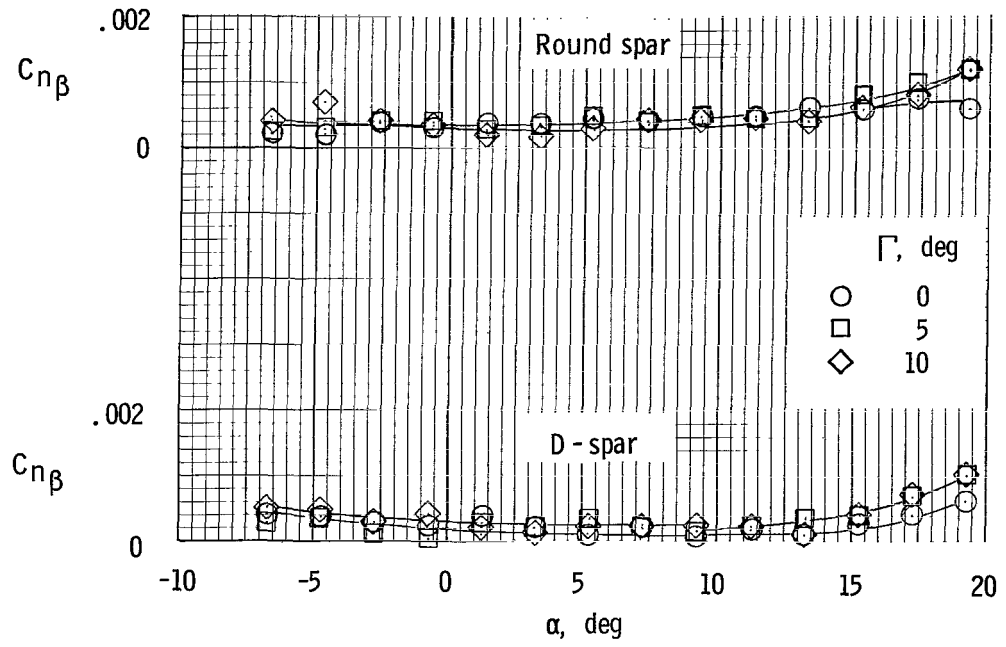
(c)  $\Gamma = 10^0$ .

Figure 10.- Concluded.



(a) Lateral stability.

Figure 11.- Variation of lateral and directional stability parameters with angle of attack.



(b) Directional stability.

Figure 11.- Concluded.

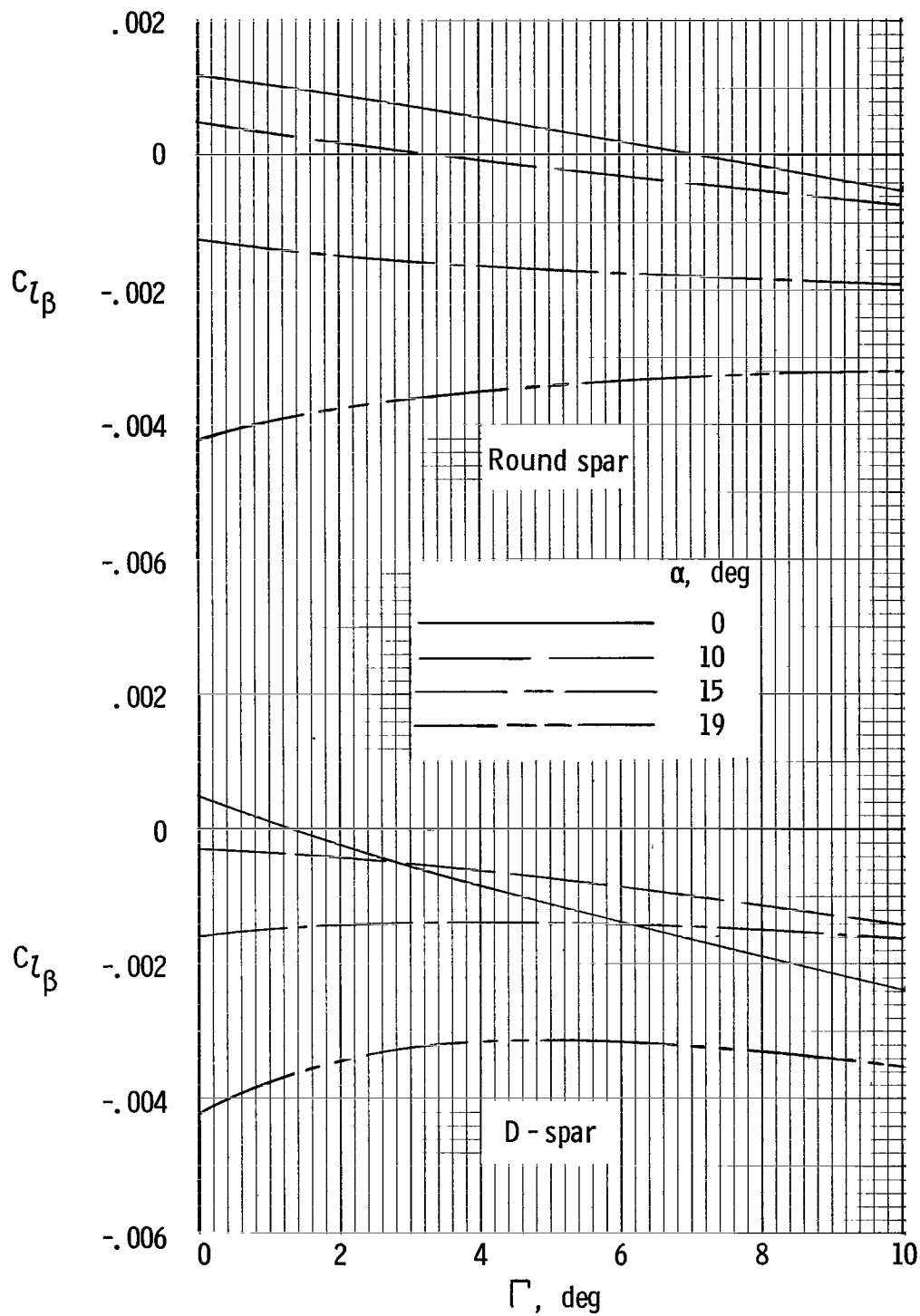


Figure 12.- Effect of geometric dihedral on effective dihedral.

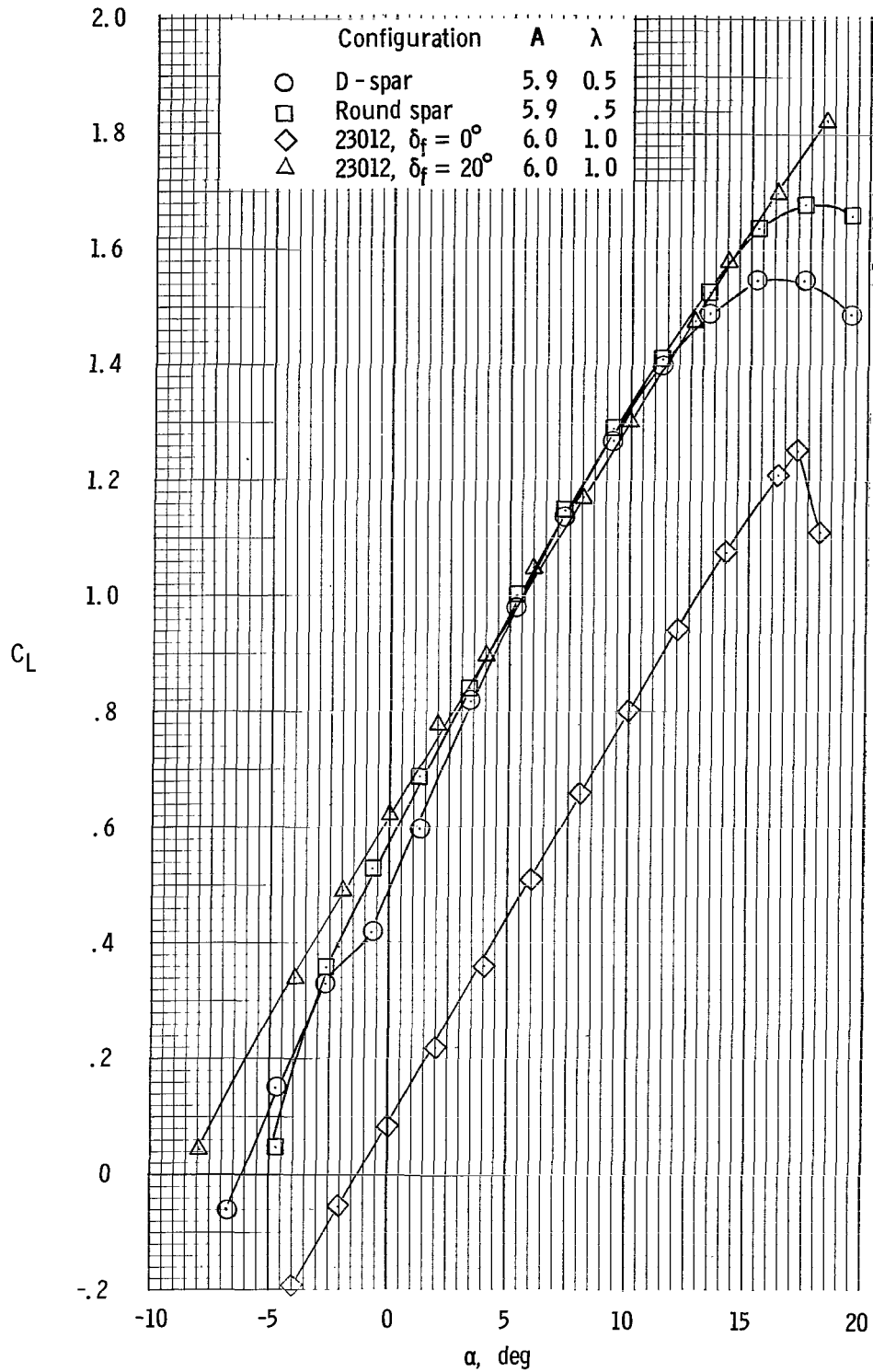


Figure 13.- Comparison of lift of sailing with that of a conventional wing.  $\Gamma = 0^\circ$ .

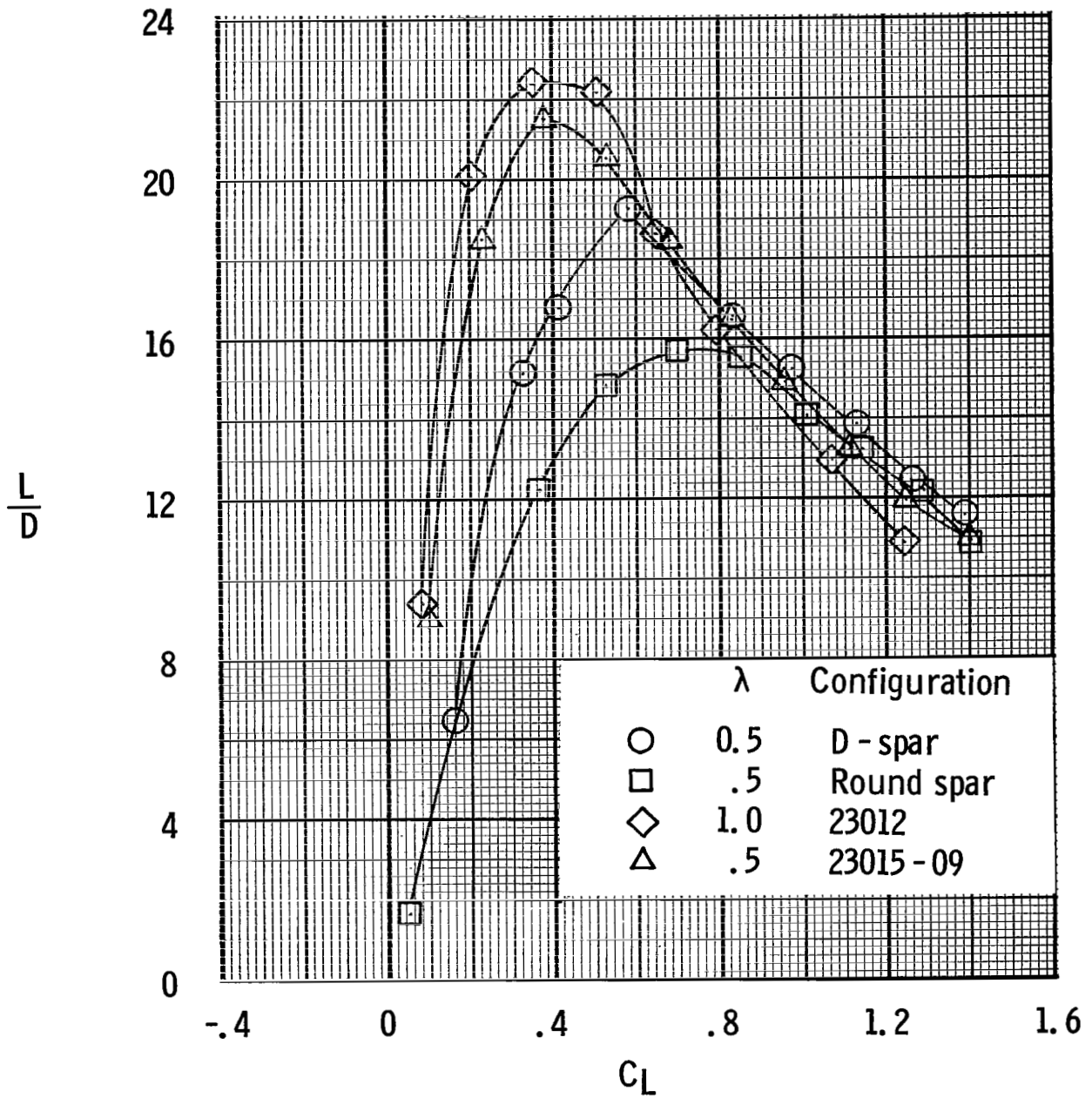


Figure 14.- Comparison of lift-drag ratio of sailing with that of conventional wings.  $\Gamma = 0^\circ$ ;  $A = 6.0$ .

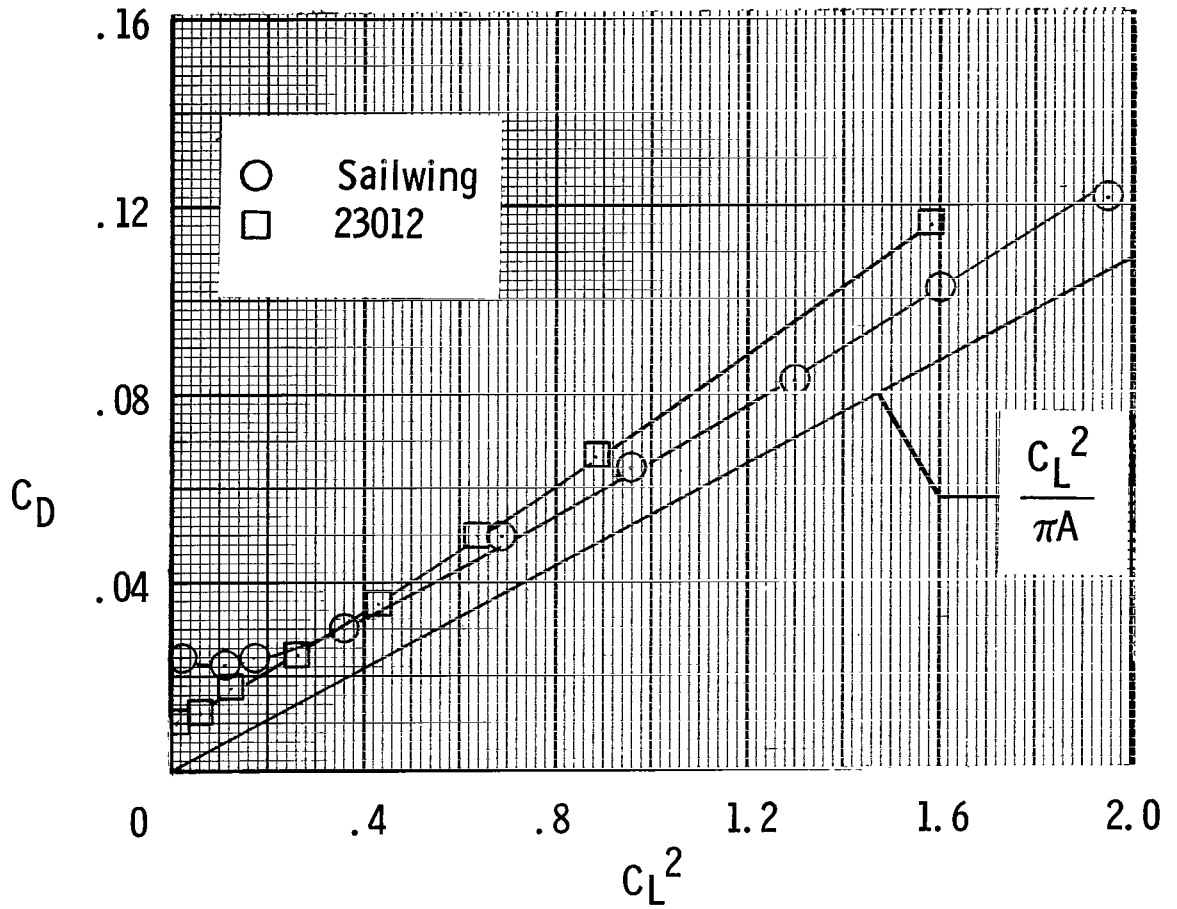


Figure 15.- Comparison of drag characteristics of sailwing with those of a conventional wing.



NATIONAL AERONAUTICS AND SPACE ADMINISTRATION  
WASHINGTON, D. C. 20546  
OFFICIAL BUSINESS

POSTAGE AND FEES PAID  
NATIONAL AERONAUTICS AND  
SPACE ADMINISTRATION

FIRST CLASS MAIL

NOV 01 20 01 30S 69033 00903  
AIR FORCE WEAPONS LABORATORY/AFWL/  
WRIGHT-PATTERSON AIR FORCE BASE, NEW MEXICO 8711

DR. LEO D. PAI, ACTING CHIEF TECH. LIC.

POSTMASTER: If Undeliverable (Section 158  
Postal Manual) Do Not Return

*"The aeronautical and space activities of the United States shall be conducted so as to contribute . . . to the expansion of human knowledge of phenomena in the atmosphere and space. The Administration shall provide for the widest practicable and appropriate dissemination of information concerning its activities and the results thereof."*

— NATIONAL AERONAUTICS AND SPACE ACT OF 1958

## NASA SCIENTIFIC AND TECHNICAL PUBLICATIONS

**TECHNICAL REPORTS:** Scientific and technical information considered important, complete, and a lasting contribution to existing knowledge.

**TECHNICAL NOTES:** Information less broad in scope but nevertheless of importance as a contribution to existing knowledge.

**TECHNICAL MEMORANDUMS:** Information receiving limited distribution because of preliminary data, security classification, or other reasons.

**CONTRACTOR REPORTS:** Scientific and technical information generated under a NASA contract or grant and considered an important contribution to existing knowledge.

**TECHNICAL TRANSLATIONS:** Information published in a foreign language considered to merit NASA distribution in English.

**SPECIAL PUBLICATIONS:** Information derived from or of value to NASA activities. Publications include conference proceedings, monographs, data compilations, handbooks, sourcebooks, and special bibliographies.

**TECHNOLOGY UTILIZATION PUBLICATIONS:** Information on technology used by NASA that may be of particular interest in commercial and other non-aerospace applications. Publications include Tech Briefs, Technology Utilization Reports and Notes, and Technology Surveys.

*Details on the availability of these publications may be obtained from:*

SCIENTIFIC AND TECHNICAL INFORMATION DIVISION  
NATIONAL AERONAUTICS AND SPACE ADMINISTRATION  
Washington, D.C. 20546